

## Influencing Receptor–Ligand Binding Mechanisms with Multivalent Ligand Architecture

Jason E. Gestwicki,<sup>†</sup> Christopher W. Cairo,<sup>‡</sup> Laura E. Strong,<sup>‡§</sup>  
Karolyn A. Oetjen,<sup>†</sup> and Laura L. Kiessling<sup>\*,†,‡</sup>

Contribution from the Departments of Biochemistry and Chemistry,  
University of Wisconsin-Madison, Madison, Wisconsin 53706

Received June 5, 2002

**Abstract:** Multivalent ligands can function as inhibitors or effectors of biological processes. Potent inhibitory activity can arise from the high functional affinities of multivalent ligand–receptor interactions. Effector functions, however, are influenced not only by apparent affinities but also by alternate factors, including the ability of a ligand to cluster receptors. Little is known about the molecular features of a multivalent ligand that determine whether it will function as an inhibitor or effector. We envisioned that, by altering multivalent ligand architecture, ligands with preferences for different binding mechanisms would be generated. To this end, a series of 28 ligands possessing structural diversity was synthesized. This series provides the means to explore the effects of ligand architecture on the inhibition and clustering of a model protein, the lectin concanavalin A (Con A). The structural parameters that were varied include scaffold shape, size, valency, and density of binding elements. We found that ligands with certain architectures are effective inhibitors, but others mediate receptor clustering. Specifically, high molecular weight, polydisperse polyvalent ligands are effective inhibitors of Con A binding, whereas linear oligomeric ligands generated by the ring-opening metathesis polymerization have structural properties that favor clustering. The shape of a multivalent ligand also influences specific aspects of receptor clustering. These include the rate at which the receptor is clustered, the number of receptors in the clusters, and the average interreceptor distance. Our results indicate that the architecture of a multivalent ligand is a key parameter in determining its activity as an inhibitor or effector. Diversity-oriented syntheses of multivalent ligands coupled with effective assays that can be used to compare the contributions of different binding parameters may afford ligands that function by specific mechanisms.

Natural and synthetic multivalent ligands can function as potent inhibitors or effectors of biological processes.<sup>1</sup> Because they present multiple copies of a receptor-binding element, multivalent ligands can bind to receptors with high avidity and specificity, thereby serving as powerful *inhibitors*.<sup>2–9</sup> Additionally, multivalent ligands can be potent *effectors* that promote a specific biological response via signal transduction.<sup>1,10,11</sup> One unique determinant of effector function is the ability to dimerize

or oligomerize receptors.<sup>12–14</sup> Thus, the potency of a multivalent ligand can depend on the mechanism of action by which it operates. For example, the effectiveness of a multivalent vaccine is influenced by its ability to cluster cell surface receptors,<sup>15</sup> but the activity of an inhibitor of the pentameric Shiga-like toxins depends on its ability to occupy multiple binding sites.<sup>16,17</sup> Understanding what type of ligands function as potent inhibitors and which act as effectors could aid in the development of multivalent displays designed for particular purposes.

Monovalent ligands have access to a limited number of binding mechanisms. These ligands typically bind to a single receptor or, less commonly, dimerize receptors via two receptor-binding faces (Figure 1). Multivalent ligands, conversely, can interact with receptors via many possible mechanisms. These include through the chelate effect, subsite binding, steric stabilization, statistical rebinding, and receptor clustering (Figure

\* To whom correspondence should be addressed. Telephone: (608) 262-0541. Fax: (608) 265-0764. E-mail: kiessling@chem.wisc.edu.

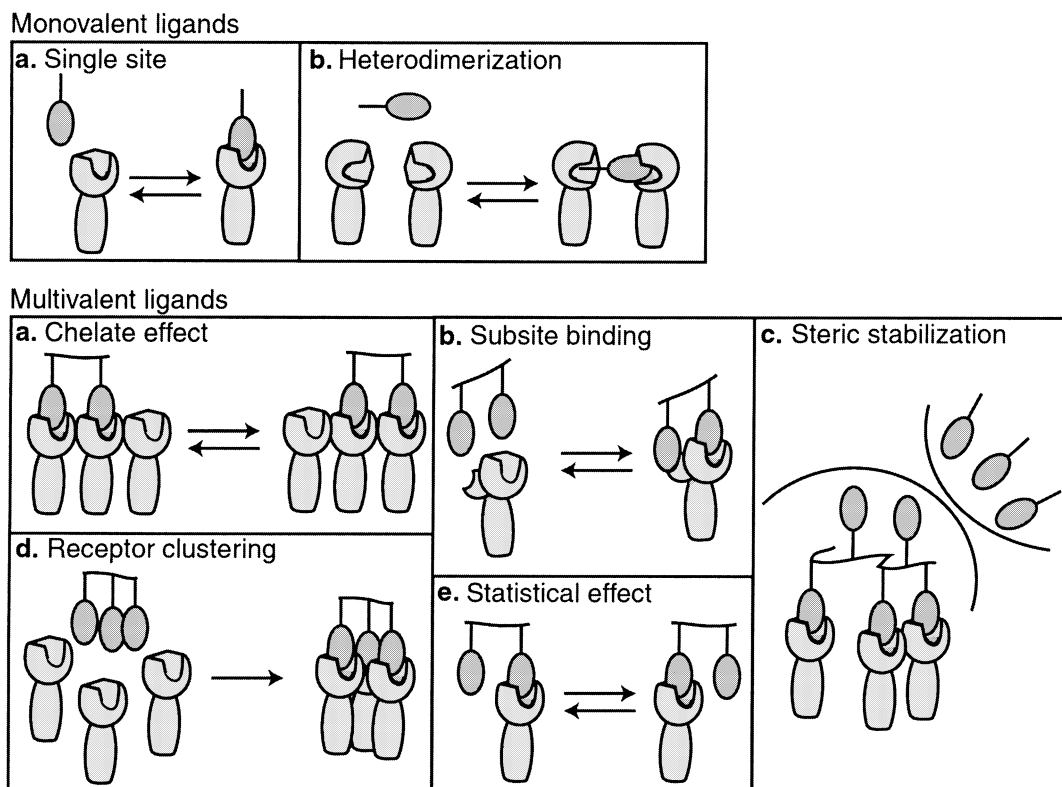
<sup>†</sup> Department of Biochemistry, University of Wisconsin-Madison.

<sup>‡</sup> Department of Chemistry, University of Wisconsin-Madison.

<sup>§</sup> Present address: Quintessence Biosciences, University Research Park, 505 South Rosa Road, Madison, WI 53719.

- (1) Kiessling, L. L.; Gestwicki, J. E.; Strong, L. E. *Curr. Opin. Chem. Biol.* **2000**, *4*, 696–703.
- (2) Mammen, M.; Choi, S.-K.; Whitesides, G. M. *Angew. Chem., Int. Ed.* **1998**, *37*, 2755–2794.
- (3) Kiessling, L. L.; Pohl, N. L. *Chem. Biol.* **1996**, *3*, 71–77.
- (4) Roy, R. *Curr. Opin. Struct. Biol.* **1996**, *6*, 692–702.
- (5) Lee, Y. C.; Lee, R. T. *Acc. Chem. Res.* **1995**, *28*, 321–327.
- (6) Bovin, N. V. *Glycoconjugate J.* **1998**, *15*, 431–446.
- (7) Houseman, B. T.; Mrksich, M. In *Host–Guest Chemistry*; 2002; Vol. 218, pp 1–44.
- (8) Lindhorst, T. K. In *Host–Guest Chemistry*; 2002; Vol. 218, pp 201–235.
- (9) Lundquist, J. J.; Toone, E. J. *Chem. Rev.* **2002**, *102*, 555–578.
- (10) Bertozzi, C. R.; Kiessling, L. L. *Science* **2001**, *291*, 2357–2364.
- (11) Clemons, P. A. *Curr. Opin. Chem. Biol.* **1999**, *3*, 112–115.

- (12) Klemm, J. D.; Schreiber, S. L.; Crabtree, G. R. *Annu. Rev. Immunol.* **1998**, *16*, 569–592.
- (13) Heldin, C.-H. *Cell* **1995**, *80*, 213–223.
- (14) Germain, R. N. *Curr. Biol.* **1997**, *7*, R640–644.
- (15) Germain, R. N. *Int. J. Technol. Assessment Health Care* **1994**, *10*, 81–92.
- (16) Kitov, P. I.; Sadowska, J. M.; Mulvey, G.; Armstrong, G. D.; Ling, H.; Pannu, N. S.; Read, R. J.; Bundle, D. R. *Nature* **2000**, *403*, 669–672.
- (17) Fan, E.; Zhang, Z.; Minke, W. E.; Hou, Z.; Verlinde, C. L. M. J.; Hol, W. G. J. *J. Am. Chem. Soc.* **2000**, *122*, 2663–2664.



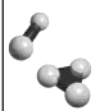
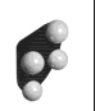
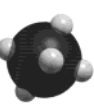

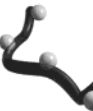
**Figure 1.** Mechanisms of ligand binding. Monovalent ligands typically (a) bind a single protein or (b) mediate heterodimerization. Multivalent ligands possess multiple copies of a recognition element presented from the same scaffold, which allows a variety of additional mechanistic options: (a) Chelate effect. Contacts between the multivalent ligand and multiple receptors decrease the off-rate and increase functional affinity. (b) Subsite binding. This is a type of chelation that involves secondary binding interactions in regions of the receptor other than the primary binding site. (c) Steric stabilization. The size of the multivalent material sterically prevents further interactions with ligands. (d) Receptor clustering. The proximity or orientation of the clustered receptors are altered by multivalent ligand binding, which can effect the signaling functions of the receptors. (e) Statistical effects. Rebinding of the multivalent ligand is favored by the high local concentration of binding elements.

1).<sup>1,2</sup> Because the structural complexity of multivalent macromolecules is greater than that of monovalent ligands, we hypothesize that the binding modes available to a multivalent ligand result from its architecture.<sup>18</sup> Consistent with this hypothesis, altering a single structural feature of a multivalent ligand, such as its valency,<sup>19–24</sup> density of binding epitopes,<sup>25–29</sup> or arrangement of binding sites,<sup>30–34</sup> can change its activity. However, because of the diversity of binding modes available to multivalent ligands, altering individual structural characteristics is unlikely to produce ligands that function by different mechanisms. To identify compounds that act by specific binding modes, new approaches that sample broad structural combinations are required.

To study the impact of multivalent ligand architecture, we utilized a common recognition element and then explored how changes in its presentation influence biological recognition. Rather than varying a single structural parameter, however, we altered the overall architecture of the multivalent ligands. This approach bears similarity to that used in combinatorial chemistry and small molecule diversity-oriented synthetic methods.<sup>35–40</sup> A critical advantage of these methods is that they allow the sampling of many compounds with varied structural characteristics.<sup>35,41,42</sup> Similarly, we envisioned that a collection of

- (18) Kiessling, L. L.; Strong, L. E.; Gestwicki, J. E. *Annu. Rep. Med. Chem.* **2000**, *35*, 321–330.  
 (19) Gestwicki, J. E.; Kiessling, L. L. *Nature* **2002**, *415*, 81–84.  
 (20) Cochran, J. R.; Stern, L. J. *Chem. Biol.* **2000**, *7*, 683–696.  
 (21) Gestwicki, J. E.; Strong, L. E.; Kiessling, L. L. *Chem. Biol.* **2000**, *7*, 583–591.  
 (22) Kanai, M.; Mortell, K. H.; Kiessling, L. L. *J. Am. Chem. Soc.* **1997**, *119*, 9931–9932.  
 (23) Dintzis, H. M.; Dintzis, R. Z.; Vogelstein, B. *Proc. Natl. Acad. Sci. U.S.A.* **1976**, *73*, 3671–3675.  
 (24) Woller, E. K.; Cloninger, M. J. *Org. Lett.* **2002**, *4*, 7–10.  
 (25) Horan, N.; Yan, L.; Isobe, H.; Whitesides, G. M.; Kahne, D. *Proc. Natl. Acad. Sci. U.S.A.* **1999**, *96*, 11782–11786.  
 (26) Maheshwari, G.; Brown, G.; Lauffenburger, D. A.; Wells, A.; Griffith, L. G. *J. Cell Sci.* **2000**, *113*, 1677–1686.  
 (27) Krantz, M. J.; Holtzman, N. A.; Stowell, C. P.; Lee, Y. C. *Biochemistry* **1976**, *15*, 3963–3968.  
 (28) Allen, J. R.; Harris, C. R.; Danishefsky, S. J. *J. Am. Chem. Soc.* **2001**, *123*, 1890–1897.  
 (29) Cairo, C. W.; Gestwicki, J. E.; Kanai, M.; Kiessling, L. L. *J. Am. Chem. Soc.* **2002**, *124*, 1615–1619.

- (30) Reuter, J. D.; Myc, A.; Hayes, M. M.; Gan, Z.; Roy, R.; Qin, D.; Yin, R.; Piehler, L. T.; Esfand, R.; Tomalia, D. A.; Baker, J. R., Jr. *Bioconjugate Chem.* **1999**, *10*, 271–278.  
 (31) Roy, R.; Page, D.; Perez, S. F.; Bencomo, V. V. *Glycoconjugate J.* **1998**, *15*, 251–263.  
 (32) Bruehl, R. E.; Dasgupta, F.; Katsumoto, T. R.; Tan, J. H.; Bertozzi, C. R.; Spevak, W.; Ahn, D. J.; Rosen, S. D.; Nagy, J. O. *Biochemistry* **2001**, *40*, 5964–5974.  
 (33) Kudryashov, V.; Glunz, P. W.; Williams, L. J.; Hintermann, S.; Danishefsky, S. J.; Lloyd, K. O. *Proc. Natl. Acad. Sci. U.S.A.* **2001**, *98*, 3264–3269.  
 (34) Reddy, J. A.; Dean, D.; Kennedy, M. D.; Low, P. S. *J. Pharm. Sci.* **1999**, *88*, 1112–1118.  
 (35) Schreiber, S. L. *Science* **2000**, *287*, 1964–1969.  
 (36) Kubota, H.; Lim, J.; Depew, K. M.; Schreiber, S. L. *Chem. Biol.* **2002**, *9*, 265–276.  
 (37) Micalizio, G. C.; Schreiber, S. L. *Angew. Chem., Int. Ed.* **2002**, *41*, 152–154.  
 (38) Stavenger, R. A.; Schreiber, S. L. *Angew. Chem., Int. Ed.* **2001**, *40*, 3417–3421.  
 (39) Ellman, J. A.; Gallop, M. A. *Curr. Opin. Chem. Biol.* **1998**, *2*, 317–319.  
 (40) Spaller, M. R.; Burger, M. T.; Fardis, M.; Bartlett, P. A. *Curr. Opin. Chem. Biol.* **1997**, *1*, 47–53.  
 (41) Ladner, R. C.; Ley, A. C. *Curr. Opin. Biotechnol.* **2001**, *12*, 406–410.  
 (42) *Combinatorial Chemistry and Molecular Diversity in Drug Discovery*; Gordon, E. M., Kerwin, J. F., Eds.; Wiley-Liss: New York, 1998.

					
	Low molecular weight compounds	Dendrimers (PAMAM)	Globular proteins (BSA)	Linear polymers (from ROMP)	Polydisperse polymers (PEMA)
Size: (Da)	small (600–700)	small (1,500–7,500)	large (~250,000)	medium (3,000–34,000)	large (~100,000)
Maximum Valency:	low (2–3)	variable (4–16)	intermediate (15–20)	variable (5–100)	high (700)

**Figure 2.** General classes of multivalent ligands used in this study and some of their general features.

multivalent ligands that vary in multiple architectural features could be generated by diversifying the scaffolds (Figure 2) used to present the receptor-binding elements. The features we explored include the overall shape and size of the ligand and the density and number of its receptor-binding elements.<sup>18</sup> By varying these parameters, we anticipated that ligands acting by distinct binding mechanisms could be identified.

The model protein we studied is the tetrameric plant lectin, concanavalin A (Con A). Con A binds  $\alpha$ -linked manno- and glucopyranosides, and it can interact with cell surface glycoproteins. A number of multivalent inhibitors of Con A-binding events have been identified.<sup>4,22,24,43,44</sup> Con A not only can bind cell surface glycoproteins but also can act as an effector by clustering them. Specifically, it is a potent mitogen and activator of apoptotic signaling pathways.<sup>45–47</sup> Moreover, Con A can be clustered by multivalent ligands,<sup>48–52</sup> which makes it an excellent model for examining ligand-promoted oligomerization. Thus, we could utilize Con A to compare both effector and inhibitor activities.

Numerous assays have been used to examine either Con A inhibition or clustering.<sup>29,43,44,49,53–55</sup> We anticipated that these could be used as a springboard for the development of assays that assess the mechanistic origins of inhibitor and effector functions. An additional criterion for our multivalent ligand assays is that they could be conducted in a high-throughput format. With such assays, the mechanisms of action of a wide range of multivalent ligands could be determined. Here, we

report the results of initial studies investigating the effects of multivalent ligand architecture on receptor binding.

## Results

**Design and Synthesis of Multivalent Ligands.** The central scaffold from which multiple receptor-binding elements are displayed influences the size, shape, and flexibility of a multivalent ligand.<sup>18</sup> To explore the effects of scaffold structure on receptor inhibition and clustering, structurally diverse scaffolds were used to generate multivalent ligands. These scaffolds, which are readily available, were selected to ensure broad structural variability. The multivalent displays fell into five general classes (Figures 2 and 3).

**1. Low Molecular Weight Compounds.** This class is composed of dimeric and trimeric displays of low molecular mass (<1000 Da).<sup>11</sup> These compounds typically only display a few recognition elements (<5), and the maximum separation between binding epitopes is often less than 10 Å.

**2. Dendrimers.** Glycodendrimers have defined valencies, but their shape and valency are dependent on their generation.<sup>24,31,56–60</sup> Their structures are thought to be compact and globular in solution.<sup>61</sup> Because of their shape and physical characteristics, dendrimers are viewed as protein mimetics and are being pursued as protein-like materials for biotechnological applications. In our studies, this class is represented by polyaminoamide (PAMAM) dendrimers.<sup>62</sup>

**3. Globular Proteins.** Proteins are commonly used as carriers for the multivalent presentation of antigens in vaccines.<sup>63</sup> Surface lysine residues are typically randomly modified by a recognition element to yield the final ligand. The resulting materials have undefined epitope presentation. Bovine serum albumin (BSA) is the representative of this class of scaffolds that was used in our studies.

**4. Linear Polymers of Defined Lengths.** This class is represented by polymers generated by ring-opening metathesis polymerization (ROMP).<sup>64,65</sup> The polymers employed are of intermediate size; their molecular mass ranges from 1 to 30 kDa, and they span approximately 20–500 Å.<sup>22</sup> For our studies, these materials are generally composed of 5–100 monomer units.<sup>22,66,67</sup> Relating activity to ligand structure is simplified because these materials can possess low polydispersity indices (PDIs).<sup>22,68</sup> Structural variation within this class is accessible by a range of synthetic methods.<sup>69–71</sup>

**5. Polydisperse Polymers.** In our studies, this class is represented by polyethylene-maleic anhydride (PEMA).<sup>72</sup> Other examples include polyacrylamide,<sup>6</sup> dextran, and polylysine

(43) Mann, D. A.; Kanai, M.; Maly, D. J.; Kiessling, L. L. *J. Am. Chem. Soc.* **1998**, *120*, 10575–10582.

(44) Corbell, J. B.; Lundquist, J. J.; Toone, E. J. *Tetrahedron: Asymmetry* **2000**, *11*, 95–111.

(45) Singh, R. S.; Tiwary, A. K.; Kennedy, J. F. *Crit. Rev. Biotechnol.* **1999**, *19*, 145–178.

(46) Cribbs, D. H.; Kreng, V. M.; Anderson, A. J.; Cotman, C. W. *Neuroscience* **1996**, *75*, 173–185.

(47) Kiss, R.; Camby, I.; Duckworth, C.; De Decker, R.; Salmon, I.; Pasteels, J.-L.; Danguy, A.; Yeaton, P. *Gut* **1997**, *40*, 253–261.

(48) Dimick, S. M.; Powell, S. C.; McMahon, S. A.; Moothoo, D. N.; Naismith, J. H.; Toone, E. J. *J. Am. Chem. Soc.* **1999**, *121*, 10286–10296.

(49) Khan, M. I.; Mandal, D. K.; Brewer, C. F. *Carbohydr. Res.* **1991**, *213*, 69–77.

(50) Burke, S. D.; Zhao, Q.; Schuster, M. C.; Kiessling, L. L. *J. Am. Chem. Soc.* **2000**, *122*, 4518–4519.

(51) Gestwicki, J. E.; Strong, L. E.; Cairo, C. W.; Boehm, F. J.; Kiessling, L. L. *Chem. Biol.* **2002**, *9*, 163–169.

(52) Sacchettini, J. C.; Baum, L. G.; Brewer, C. F. *Biochemistry* **2001**, *40*, 3009–3015.

(53) Ballerstadt, R.; Schultz, J. S. *Anal. Chim. Acta* **1997**, *345*, 203–212.

(54) Gestwicki, J. E.; Strong, L. E.; Kiessling, L. L. *Angew. Chem., Int. Ed.* **2000**, *39*, 4567–4570.

(55) Oppenheimer, S. B. In *Concanavalin A as a Tool*; Bittiger, H., Schnebli, H. P., Eds.; John Wiley & Sons, Ltd.: London, 1976; pp 293–299.

(56) Zimmerman, S. C.; Lawless, L. J. In *Dendrimers IV*; 2001; Vol. 217, pp 95–120.

(57) Moore, J. S. *Curr. Opin. Solid State Mater. Sci.* **1996**, *1*, 777–788.

(58) Pollak, K. W.; Leon, J. W.; Frechet, J. M. J.; Maskus, M.; Abruna, H. D. *Chem. Mater.* **1998**, *10*, 30–38.

(59) Jayaraman, N.; Nepogodiev, S. A.; Stoddart, J. F. *Chem.—Eur. J.* **1997**, *3*, 1193–1199.

(60) Rockendorf, N.; Lindhorst, T. K. In *Dendrimers IV*; 2001; Vol. 217, pp 201–238.

(61) Perec, V.; Cho, W.-D.; Ungar, G. *J. Am. Chem. Soc.* **2000**, *122*, 10273–10281.

(62) Tomalia, D. A.; Naylor, A. M.; Goddard, W. A. *Angew. Chem., Int. Ed. Engl.* **1990**, *29*, 138–175.

(63) Arnon, R.; Vanregenmortel, M. H. V. *FASEB J.* **1992**, *6*, 3265–3274.

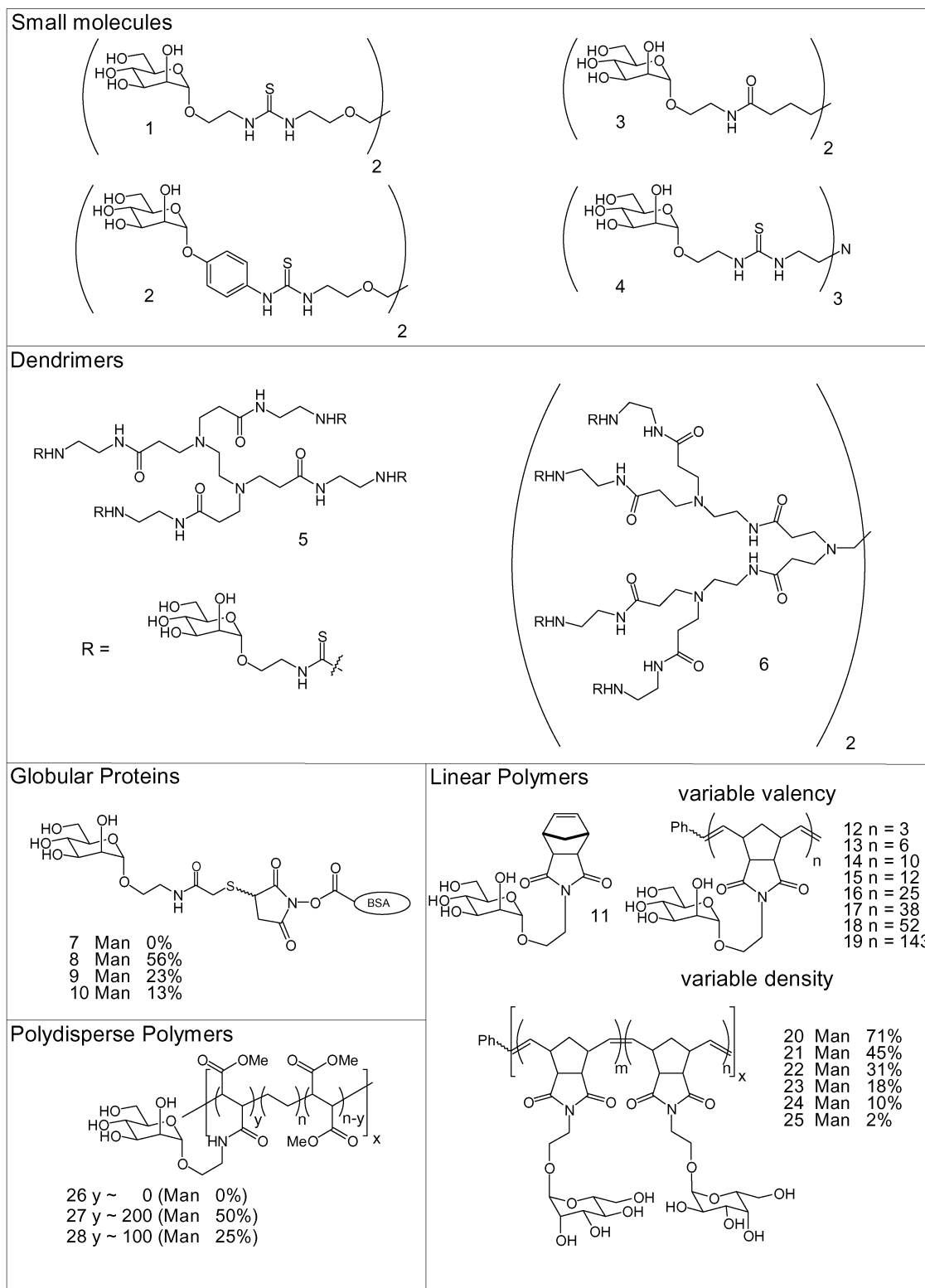
(64) Kiessling, L. L.; Strong, L. E. *Top. Organomet. Chem.* **1998**, *1*, 199–231.

(65) Trnka, T. M.; Grubbs, R. H. *Acc. Chem. Res.* **2001**, *34*, 18–29.

(66) Fraser, C.; Grubbs, R. H. *Macromolecules* **1995**, *28*, 7248–7255.

(67) Schrock, R. R.; Lee, J. K.; Odell, R.; Oskam, J. H. *Macromolecules* **1995**, *28*, 5933–5940.

(68) Lynn, D. M.; Mohr, B.; Grubbs, R. H. *J. Am. Chem. Soc.* **1998**, *120*, 1627–1628.



**Figure 3.** Chemical structures of ligands. These include small-molecule dimers (**1–3**) and a trimer (**4**); PAMAM dendrimers of generation zero (**5**) and one (**6**); mannosylated BSA (**8–10**); and scaffold (**7**). For BSA conjugates, the percent mannose derivative incorporation (man %) is the average number of mannose residues conjugated to the BSA compared to the total number of available activated surface residues. The average valency of the BSA-derived multivalent ligands are as follows: 10 mannose residues per scaffold (**8**), 5 residues per scaffold (**9**), and 2 residues per scaffold (**10**). Other ligands include monomer **11**, which was used to generate polymers **12–19** that vary in valency ( $n$ ) by ROMP. Variable densities of mannose- and galactose-derivatized monomers ( $m$  and  $n$ ) were used to create ROMP-derived ligands (**20–25**) with lengths ( $x$ ) similar to that of compound **19** (approximately 120 monomer units). PEMA was used to generate a scaffold (**26**) and mannosylated ligands (**27–28**). The number of mannose residues per polymer is approximately 200 for compound **27** and 100 for compound **28**, and the number of randomly interdispersed ethylene spacers ( $n$ ) is approximately 400 (see Experimental Materials and Methods section).

derivatives.<sup>73</sup> These materials typically have high molecular masses and large PDIs.

A member of each class of scaffold was converted to a multivalent ligand by conjugation of multiple copies of the Con A-binding element mannose.  $\alpha$ -Linked mannosides are low affinity ligands ( $K_d \approx 10^{-3}$  M) for Con A, and a substituent at the anomeric position can be used to append them to a scaffold of interest.<sup>22,74–76</sup> Mannose derivatives containing an anomeric substituent bearing either a primary amino group or an isothiocyanate group were used to generate the multivalent displays **1–6**, **8–10**, **12–25**, and **27–28** (Figure 3; see Experimental Materials and Methods section). The monovalent ligand **11** and the underivatized scaffolds **7** and **26** served as control compounds in the binding studies.

The number of mannose residues displayed on the linear defined polymers (**11–25**), polydisperse polymers (**26–28**), and globular protein conjugates (**7–10**) was varied. Variation in the number of mannose residues on the ROMP-derived linear defined polymers was controlled in two ways. First, the polymer length was altered.<sup>22,68</sup> This results in materials that vary in valency but possess a uniform density of mannose residues (**11–19**). Additionally, a second series of ROMP-derived ligands was generated by holding the polymer length constant and varying the density of mannose residues (**20–25**).<sup>29</sup> These were synthesized by varying the molar ratio of galactose- and mannose-bearing monomers in the polymerization reactions. Because galactose is not a ligand for Con A, copolymerization of these monomers results in a series of ligands that vary in the density of their Con A-binding elements. Variable density ligands also were generated from polydisperse polymers and globular protein scaffolds. For these scaffolds, density control was achieved by changing the mole fraction of the mannose derivative used in the conjugation reactions.<sup>27</sup> Thus, multivalent ligands with different valencies and densities of mannose residues were produced.

We required a uniform method for comparing the potencies of diverse ligands. To this end, we determined the saccharide content of the purified ligands by sulfuric acid/phenol treatment.<sup>77</sup> This method provided the means to determine the mannose concentrations of all of our ligand solutions, and the activity of the multivalent ligands could be compared using these mannose concentrations. Because of the presence of galactose-bearing monomer units in ligands **20–25**, the concentration of mannose in solutions of these ligands was calculated by multiplying the total saccharide concentration by the percent of mannose-bearing monomer. Spectroscopic data indicate that the relative ratios of galactose- and mannose-substituted monomers incorporated into the polymer products correlate with the ratios used in the polymerization reactions.

- (69) Strong, L. E.; Kiessling, L. L. *J. Am. Chem. Soc.* **1999**, *121*, 6193–6196.  
(70) Gordon, E. J.; Gestwicki, J. E.; Strong, L. E.; Kiessling, L. L. *Chem. Biol.* **2000**, *7*, 9–16.  
(71) Maynard, H. D.; Okada, S. Y.; Grubbs, R. H. *J. Am. Chem. Soc.* **2001**, *123*, 1275–1279.  
(72) Lu, B.; Chung, T. C. *J. Polym. Sci., Polym. Chem. Ed.* **2000**, *38*, 1337–1343.  
(73) Thoma, G.; Patton, J. T.; Magnani, J. L.; Ernst, B.; Ohrlein, R.; Duthaler, R. O. *J. Am. Chem. Soc.* **1999**, *121*, 5919–5929.  
(74) Williams, B.; Chervenak, M.; Toone, E. J. *J. Biol. Chem.* **1992**, *267*, 22907–22911.  
(75) Weatherman, R. V.; Kiessling, L. L. *J. Org. Chem.* **1996**, *61*, 534–538.  
(76) Goldstein, I. J.; Poretz, R. D. In *The Lectins: Properties, Functions and Applications in Biology and Medicine*; Liener, I. E., Sharon, N., Goldstein, I. J., Eds.; Academic Press: Orlando, FL, 1986; p 35.  
(77) Dubois, M.; Gilles, K. A.; Hamilton, J. K.; Rebers, P. A.; Smith, F. *Anal. Chem.* **1956**, *28*, 350–356.

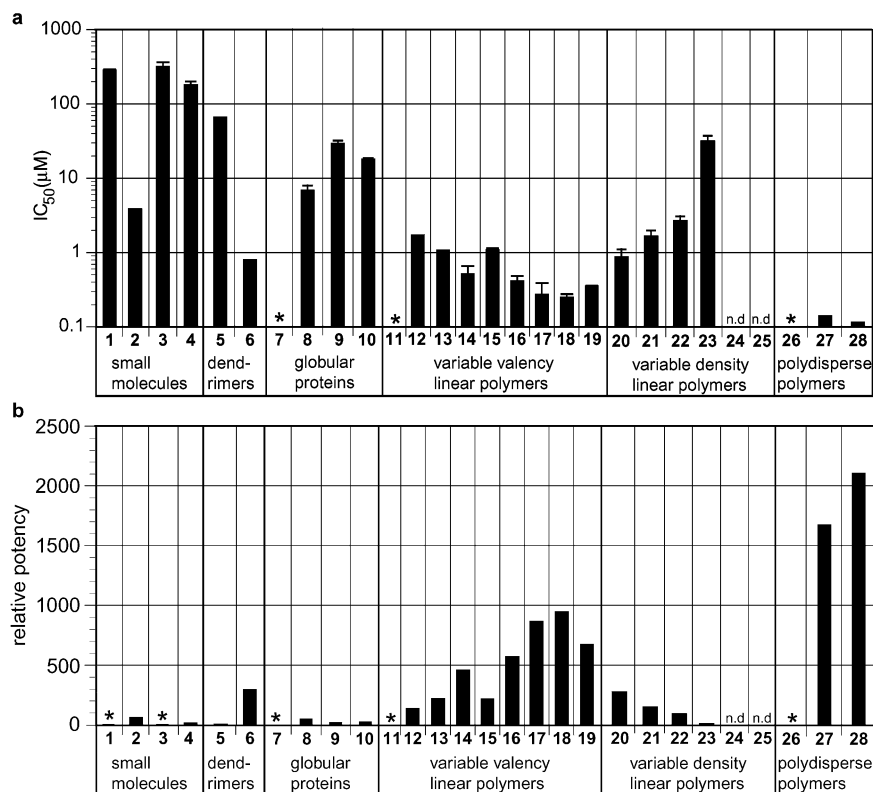
**Design of Assays for Exploring Multivalent Ligand-Binding Mechanisms.** Previous investigations of multivalent ligand–receptor interactions have typically utilized single assays for evaluating ligand activity.<sup>2–9</sup> A single assay, however, often only reports on one aspect of multivalent binding. Solid-phase binding assays, for example, are well suited for exploring binding inhibition, but they do not distinguish effects arising from receptor clustering.<sup>78</sup> Assays appropriate for the study of receptor clustering, which can be an important determinant of effector function, have been described.<sup>29</sup> These include quantitative precipitation,<sup>49</sup> turbidity measurements,<sup>31</sup> and quenching of fluorescence emission,<sup>50,51,79</sup> and they provide insight into specific aspects of clustering. For example, fluorescence quenching reports on the average intermolecular distances between receptors present in a cluster; therefore, it is a measure of receptor proximity.<sup>79</sup> No single assay can elucidate the contributions of ligand structure to multivalent binding mechanisms. Moreover, if the binding of diverse multivalent ligands is to be assessed, assays that can be carried out in a high throughput format are needed. To fully investigate multivalent ligand function broadly, we employed four different assays.

**Solid-Phase Binding Assay.** Multivalent ligands are often generated in an effort to identify potent inhibitors.<sup>2,4</sup> To determine how the structural features of a multivalent ligand influence inhibitory activity, a solid-phase binding assay to evaluate the ability of ligands **1–28** to block Con A binding was developed.<sup>78</sup> Fluorescein-labeled Con A was added to polystyrene wells to which a mannose derivative had been attached covalently. Inclusion of **1–28** in the fluoresceinated Con A solutions resulted in an inhibition of lectin binding to immobilized mannose residues. From the intensity of the fluorescence emission signals retained on the plate at various inhibitor concentrations, the  $IC_{50}$  values for each of the ligands were determined (Figure 4a). The potency of each ligand relative to methyl  $\alpha$ -D-mannopyranoside ( $\alpha$ MeMan, Figure 4b) was measured. The inhibitory potencies of the ligands were compared on the basis of their mannose residue concentrations.

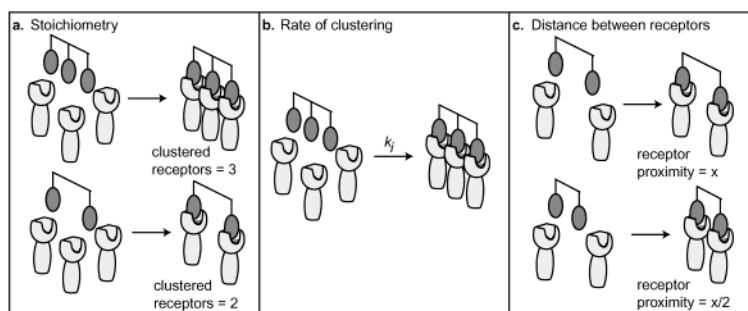
We compared the relative potencies of the ligands derived from structurally diverse scaffolds. The polymers derived from either defined or polydisperse backbones were the most effective inhibitors. Linear defined polymer **15** was a 1000-fold better inhibitor of fluorescent Con A binding than  $\alpha$ MeMan, and the polydisperse polymer with the highest binding epitope density (**19**) was the most effective: 2000-fold more potent than  $\alpha$ MeMan. The first generation dendrimer **6** was also an effective inhibitor of Con A binding (290-fold more potent than  $\alpha$ MeMan). The globular protein conjugates (**8–10**), however, were only modest inhibitors of fluoresceinated Con A binding with relative potencies between 9- and 38-fold better than that of  $\alpha$ MeMan. Conversely, the low molecular weight di- and trivalent ligands (**1–4**) and the dendrimer **5** poorly inhibited the binding of fluoresceinated Con A. Thus, the mannose-substituted polymers, especially those of high molecular weight, are the most effective inhibitors of Con A; the low molecular weight ligands, dendrimers, and globular proteins are less potent.

**Clustering Assays.** Receptor clustering can be a critical determinant of effector function.<sup>12–14</sup> Here, we examined three

- (78) McCoy, J. P., Jr.; Varani, J.; Goldstein, I. J. *Anal. Biochem.* **1983**, *130*, 437–444.  
(79) Matko, J.; Edidin, M. *Methods Enzymol.* **1997**, *278*, 444–462.



**Figure 4.** Results of solid-phase binding assays. (a) Nonlinear fits to a standard dose–response curve were used to determine the  $IC_{50}$  values based on data generated from seven concentrations of ligand. The concentrations of all ligands are based on their mannose concentration. The error bars represent the standard deviation. Asterisks represent those compounds that were unable to inhibit Con A binding ( $IC_{50} > 1$  mM). (b) The potency of each ligand is shown relative to the canonical Con A ligand, methyl- $\alpha$ -D-mannopyranoside ( $\alpha$ MeMan). Asterisks represent those compounds with an  $IC_{50}$  value greater than that of  $\alpha$ MeMan. n.d. = not determined.



**Figure 5.** Factors influencing receptor clustering. Factors such as (a) the number of clustered receptors, (b) the rate of clustering, and (c) the distance between receptors might influence the productivity of and/or biological response elicited by receptor clustering.

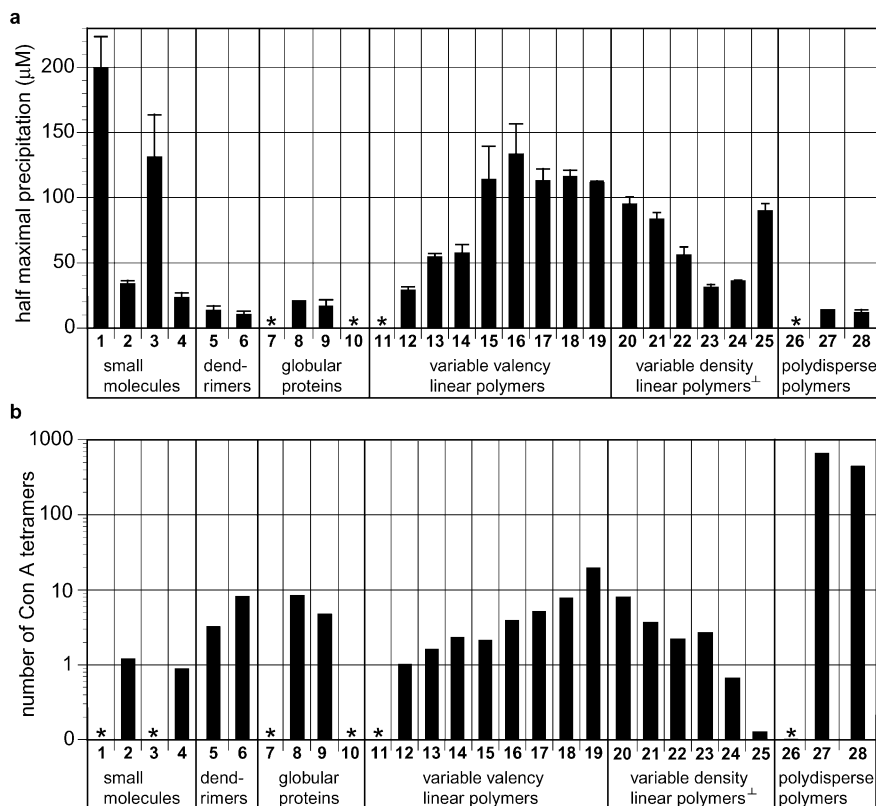
different aspects of clustering: the number of receptors included in the cluster (Figure 5a), the rate of clustering (Figure 5b), and the distance between receptors in the clusters (Figure 5c). Each of these aspects of ligand-promoted clustering was assessed in a separate assay that was tailored to predominantly report on one of them.

**Quantitative Precipitation Assay.** How effectively a ligand clusters receptors might be related to its inhibitory potency in binding assays.<sup>44,48</sup> In addition, the number of receptors in a cluster is an important determinant for multivalent ligand-induced signaling (Figure 5a).<sup>12,23</sup> To address whether scaffold structure has an effect on the stoichiometry of the resulting clusters, the number of Con A tetramers bound by each ligand was determined by using a quantitative precipitation assay.<sup>49</sup> These experiments determine the concentration of ligand required to precipitate half of the lectin from solution ( $P_{1/2}$ ,

Figure 6a). The  $P_{1/2}$  values provide a measure of the stoichiometric composition of the precipitates (Figure 6b).<sup>80</sup>

Our results reveal that the stoichiometry of Con A–ligand complexes depends on the structural class of the multivalent ligand used to initiate the clustering. The low molecular weight compounds (particularly, **2** and **4**) were effective precipitating agents in this assay ( $P_{1/2} = 34$  and  $23$   $\mu M$ , respectively), but only a 1:1 ligand–Con A stoichiometry was found in the precipitates.<sup>49</sup> Unlike the low molecular weight compounds, the dendrimers (**5–6**), globular proteins (**8–10**), and linear polymers derived from ROMP (**12–25**) afforded complexes of Con A with stoichiometries ranging from 1:1 to 1:20 (ligand to Con A). The largest Con A clusters were likely generated by the mannose-substituted polydisperse polymers (**27–28**), which can

(80) Olsen, L. R.; Dessen, A.; Gupta, D.; Sabesan, S.; Sacchettini, J. C.; Brewer, C. F. *Biochemistry* **1997**, *36*, 15073–15080.



**Figure 6.** Results of quantitative precipitation experiments. Con A was titrated with ligands at concentrations between 0.01 and 300  $\mu\text{M}$  (or 0.001–75  $\mu\text{M}$  for compounds 7–10). Each point is the average of at least two replicates performed in duplicate. (a) Nonlinear fits were used to determine the concentration required for half-maximal precipitation. The error bars represent the standard deviation. Asterisks indicate that no precipitation was observed. (b) The number of Con A tetramers bound per multivalent ligand is shown. These values were determined from the inflection point of the precipitation curves, as described previously.<sup>49,51</sup> Asterisks indicate that no precipitation was observed or that the inflection point analysis could not be performed. The marked data<sup>†</sup> are taken from ref 29.

assemble complexes containing approximately 400–600 copies of Con A tetramer for each polymer. Thus, the high molecular weight polymers were extremely effective at binding many copies of Con A, the ligands generated by ROMP were also effective, the dendrimers and globular proteins formed clusters with intermediate stoichiometries, and the low molecular weight ligands formed 1:1 complexes.

**Turbidity Assay.** Many signaling events are regulated by the rate of ligand binding (Figure 5b),<sup>81</sup> and the rate of multivalent ligand-induced receptor clustering can vary.<sup>82,83</sup> Little is known about how the structural features of a multivalent ligand influence the kinetics of ligand-induced clustering.<sup>29</sup> To address this issue, we employed a kinetic turbidity assay to investigate the effects of ligand architecture on the rate at which Con A is clustered. Multivalent ligand binding to Con A can result in the clustering and subsequent precipitation of Con A–ligand complexes. Turbidity measurements can, therefore, be used to monitor the formation of complexes in real time.<sup>31,84</sup> Ligands 1–28 were added to Con A solutions, and the turbidity of the mixture was monitored. The initial rate of precipitation ( $k_i$ , Figure 7a) was determined by linear fits to the initial portion of the data. The endpoint of precipitation was used to determine the  $t_{1/2}$  values (Figure 7b).

Multivalent ligands that possess high valency and binding epitope density most rapidly initiated Con A clustering. Those ligands with high mannose density, such as the multivalent ROMP-derived ligands (12–19), promoted the rapid precipitation of Con A ( $k_i > 0.36$  au/min,  $t_{1/2} < 12$  s). Conversely, compounds with low valencies, such as the low molecular weight compounds (1–4), the lower generation dendrimer 5, and the ligands derived from the globular proteins (8–10) generally exhibited moderate clustering rates ( $t_{1/2} > 2$  min). The ROMP-derived ligands with decreased binding epitope density (20–25) also led to decreased rates.<sup>29</sup> The shape of the scaffold was indirectly related to the kinetics of Con A clustering. The rate of precipitation of Con A induced by dendrimer 6 ( $k_i = 0.2$  au/min,  $t_{1/2} = 20$  s) was faster than that mediated by ligands that have been postulated to have similar shapes, such as the globular protein conjugates. The polydisperse polymers (27–28) were of intermediate potency ( $k_i = 0.1$  to 0.2 au/min,  $t_{1/2}$  approximately 20 s) despite the excellent inhibitory capability of these materials. Thus, the polymers derived from ROMP possess the most favorable scaffold architecture (high binding epitope density and valency) for the rapid clustering of Con A, while the other scaffolds had lesser activity.

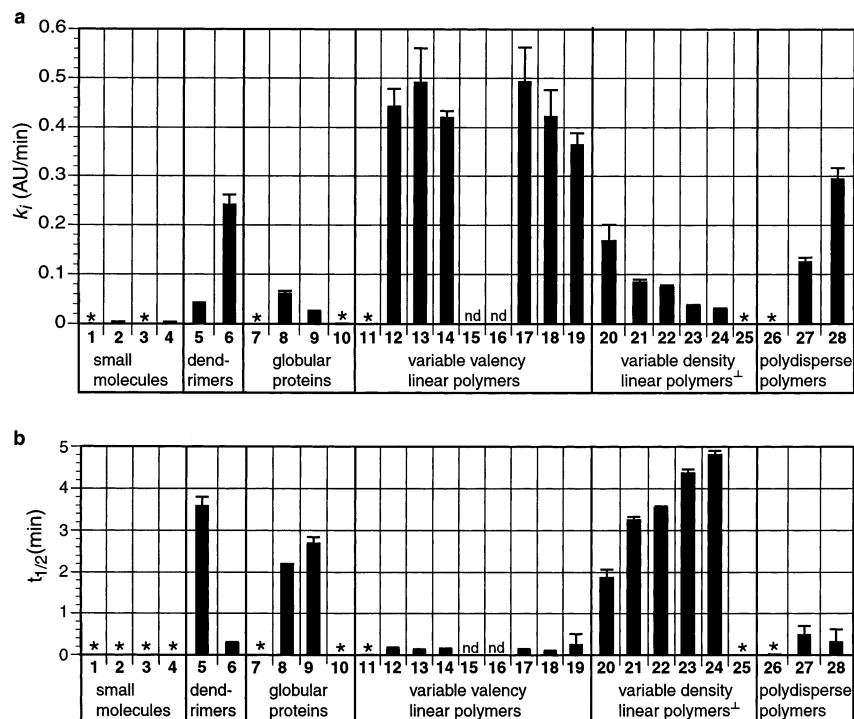
**Fluorescence Quenching Assay.** Multivalent ligands can alter the distance between receptors (Figure 5c).<sup>12,13</sup> Changes in receptor proximity can be an important determinant of receptor function. For example, the distance between erythropoietin (EPO) receptors decreases from 73 to 39 nm (ap-

(81) Germain, R. N.; Stefanova, I. *Annu. Rev. Immunol.* **1999**, *17*, 467–522.

(82) Weintraub, B. C.; Jun, J. E.; Bishop, A. C.; Shokat, K. M.; Thomas, M. L.; Goodnow, C. C. *J. Exp. Med.* **2000**, *191*, 1443–1448.

(83) Sugiyama, J. E.; Glass, D. J.; Yancopoulos, G. D.; Hall, Z. W. *J. Cell Biol.* **1997**, *139*, 181–191.

(84) Easterbrook-Smith, S. B. *Mol. Immunol.* **1993**, *30*, 637–640.

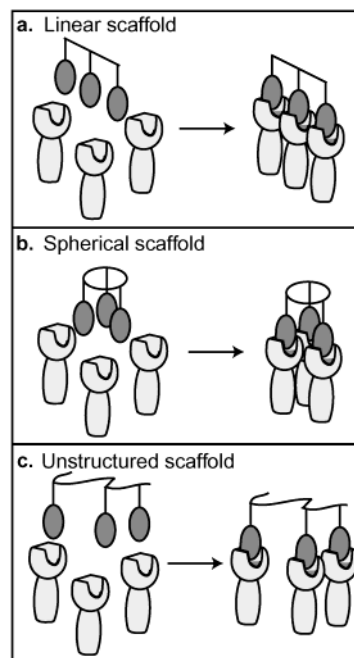


**Figure 7.** Results of turbidity experiments. Complexation was measured by monitoring  $A_{420}$  for 10 min after the addition of ligand. (a) The initial linear portion of the curve was fit to determine the initial rate of precipitation ( $k_i$ ). Each bar is the average of three replicates. The concentrations of all ligands are based on their mannose concentration. Error bars represent the standard deviation. (b) The precipitation profiles were fit to determine the time required for half-maximal precipitation ( $t_{1/2}$ ). Asterisks indicate that no precipitation was observed or that precipitation did not reach a maximal value during the 10 min incubation. nd = not determined. The marked data<sup>+</sup> are taken from ref 29.

proximately 2-fold) when bound to the activator EPO.<sup>85,86</sup> To determine how multivalent scaffold structure influences the average interreceptor distances in a complex (Figure 8), fluorescence emission quenching measurements were used.<sup>50,51</sup> Fluorescence quenching efficiency varies as the sixth power of the separation distance; therefore, a decrease in fluorescence intensity can be interpreted as either a decrease in the average distance between fluorophore-labeled proteins or an increase in the number of adjacent receptors.<sup>53,79</sup> Thus, this assay reports on receptor proximity, a relevant feature of multivalent ligand-induced clustering.

Ligands 1–28 were added to a solution of fluorescein- and rhodamine-labeled Con A. The emission intensity of fluorescein was evaluated to determine the fluorescence quenching efficiency.<sup>79</sup> Two parameters were measured: the mannose concentration required for half-maximal fluorescence quenching ( $F_{1/2}$ , Figure 9a) and the maximum percentage change in fluorescence emission ( $F_{max}$ ) compared to that of an untreated control (Figure 9b).

Our results reveal that multivalent ligand architecture is a key determinant of the proximity between clustered receptors. Generally, the fluorescence quenching induced by low molecular weight ligands (1–4) was inefficient. The exception was that observed with the hydrophobic dimer 2, which was an excellent mediator of quenching ( $F_{1/2} = 0.2 \mu\text{M}$ ,  $F_{max} = 42\%$ ). Energy transfer was minimal for complexes generated from the dendrimers and globular protein-derived ligands (8–10) ( $F_{max} <$



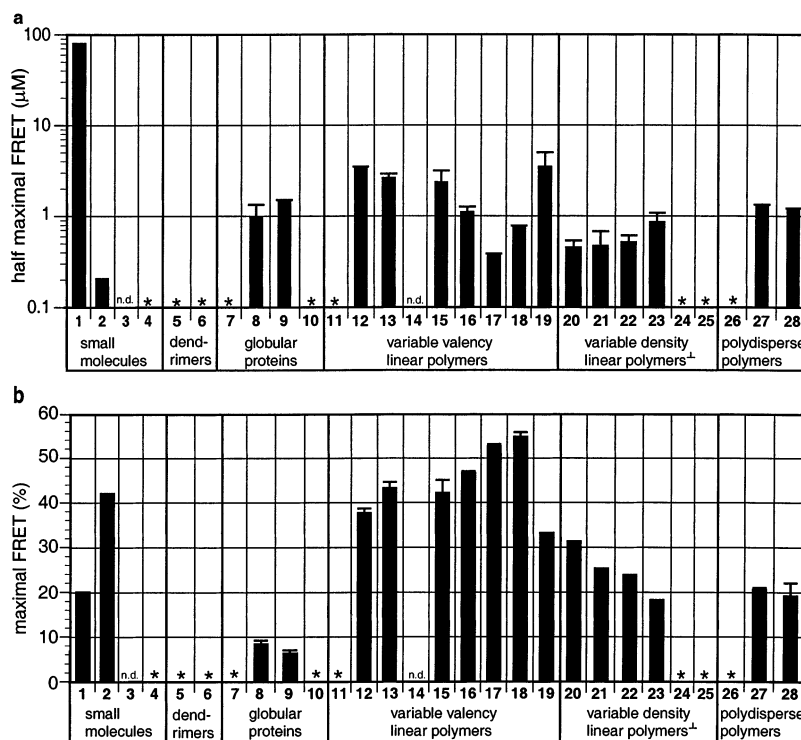
**Figure 8.** Schematic depicting the influence of multivalent ligand architecture on the distance and orientation between clustered receptors. (a) A linear scaffold imparts linear structure to a macromolecular cluster of receptors. Likewise, choosing a (b) spherical or (c) unstructured scaffold will result in the formation of distinct macromolecular assemblies.

10%). Although other assays indicate that dendrimer- and globular protein-based ligands are able to cluster Con A, the lectins in the clusters may be assembled at distances or orientations unfavorable for fluorescence quenching. In contrast, fluorescence quenching was observed in clusters formed by the

(85) Livnah, O.; Stura, E. A.; Middleton, S. A.; Johnson, D. L.; Jolliffe, L. K.; Wilson, I. A. *Science* **1999**, *283*, 987–990.

(86) Livnah, O.; Stura, E. A.; Johnson, D. L.; Middleton, S. A.; Mulcahy, L. S.; Wrighton, N. C.; Dower, W. J.; Jolliffe, L. K.; Wilson, I. A. *Science* **1996**, *273*, 464–470.





**Figure 9.** Results of fluorescence quenching experiments. Fluorescein- and rhodamine-labeled Con A samples were mixed in solution to a final concentration of 80 nM. Fluorescein emission was measured and is presented as a percentage of an untreated control. Individual titrations consist of 3 repetitions comprised of 10–12 concentrations over the range of 0.001–50  $\mu\text{M}$ . Error bars represent the standard deviation. The concentration of ligand required for (a) half-maximal change in fluorescence and (b) the maximal percent change in fluorescence are shown. The concentrations of all ligands are based on their mannose concentrations. Asterisks indicate that no change in fluorescence was observed up to 50  $\mu\text{M}$ . The marked data<sup>+</sup> are taken from ref 29.

ligands derived from polydisperse scaffolds ( $F_{\text{max}}$  of approximately 20%). The greatest quenching efficiency, however, was observed using the ligands with high binding epitope density synthesized by ROMP (12–19;  $F_{\text{max}}$  values ranged from 33 to 55%). Thus, despite the ability of the polydisperse polymers to assemble more copies of Con A per polymer, the complexes generated with ROMP-derived ligands resulted in more efficient quenching. These results indicate that the ROMP-derived ligands are especially effective at promoting Con A clustering and that the individual proteins within the clusters are positioned at distances appropriate for energy transfer ( $< 10$  nm).

## Discussion

Multivalent ligands can interact with receptors in a variety of binding modes (see Figure 1).<sup>1,2</sup> We postulated that testing diverse multivalent ligands could illuminate the binding modes underlying the activities of specific ligand architectures. To test this hypothesis, we generated multivalent ligands with diverse architectures and compared their abilities to interact with the tetrameric receptor Con A. Our results indicate that the molecular features of the multivalent ligands influence the mechanisms by which they function.

A panel of assays that report on specific parameters important in multivalent binding was employed. The assays were amenable to screening in a high throughput format. The solid-phase binding assay was used to compare relative inhibitory concentrations of each multivalent ligand. In addition, assays that report on different aspects of receptor clustering were used. These include measurements of the stoichiometry of the complexes (quantitative precipitation), the rate of clustering (turbidity), and the proximity of the receptors in the complex (fluorescence

	Low molecular weight compounds	Dendrimers (PAMAM)	Globular proteins (BSA)	Linear polymers (from ROMP)	Polydisperse polymers (PEMA)
Avidity:	+	+	++	++	+++
Rate:	+	++	+	+++	++
Cluster size:	+	++	++	++	++++
Proximity:	++	-	+	+++	++

**Figure 10.** Summary of the activity of the different classes of scaffolds. A number of pluses (+) were assigned to the activity of the different architectures. Avidity: average relative potency from solid-phase binding assay 1–200 (+), 200–1000 (++) and  $> 1000$  (+++). Turbidity: average  $k_i < 0.1$  (+) and 0.1–0.3 (++) and  $> 0.3$  (+++) au/min. Cluster size: average number of receptors  $< 2$  (+), 2–10 (++) and 10–100 (+++) and  $> 100$  (++++). Proximity: average maximum change in fluorescence emission  $< 10\%$  (+) and 10–30% (++) and  $> 30\%$  (+++). Compounds that lacked any apparent activity were not included in these analyses.

quenching). All of these assays require small sample volumes, and both the solid-phase binding and fluorescence quenching assays were performed using microtiter plates. Thus, libraries of multivalent ligands can be screened for specific mechanisms of action.

In Figure 10, the results for the different assays we employed to investigate Con A inhibition and clustering are summarized. The data suggest that ligands with high molecular masses, such as the polydisperse polymers and globular proteins, are excellent inhibitors of Con A binding. These ligands, especially the

former, bound many copies of Con A (see Figure 6). Despite their ability to interact with many copies of Con A, the kinetics of their interaction (Figure 7) were slower and the average distances of Con A tetramers in these clusters (Figure 9) were unexpectedly large. These results indicate that the high molecular weight polydisperse polymers and protein conjugates are effective inhibitors but are likely to be less potent effectors. Interestingly, the highly substituted polymers generated by ROMP had the highest activities in the assays that measure receptor clustering. These ligands are especially effective at rapidly promoting receptor clustering, a property that is important for triggering signal transduction. Moreover, within these ligand promoted clusters, the receptors were proximal, as judged by fluorescence quenching. Thus, compounds that inhibit binding are not the most active promoters of functional cluster formation. Still, our data indicate that these activities are not completely decoupled in this system.<sup>44</sup>

Our results provide insight into the most effective scaffolds for a specific mode of action. Specifically, our results suggest that clustering is the preferred mechanism by which ROMP-derived scaffolds interact with Con A. In contrast, polyvalent ligands with large globular or undefined structures were the most potent inhibitors of Con A binding, but these were not as effective at facilitating Con A clustering. Our results highlight the benefit of testing diverse scaffolds for ligand presentation, as different scaffolds may favor specific binding modes. We note that none of the ligands tested here were designed to have a specific mode of action, yet differences in their binding modes were found. We suggest applications of diversity-oriented syntheses may advance the search for scaffolds for multivalent ligands tailored for specific functions.<sup>87,88</sup>

Low molecular weight ligands were generally poor at inhibiting Con A binding in the solid-phase binding assay (see Figure 4). They also were poor clustering agents in the turbidity, quantitative precipitation, and fluorescence quenching assays (see Figures 6, 7 and 9). Although the data indicate that high-valency ligands possess the most potent activities, some low molecular weight compounds, particularly **2**, can inhibit and cluster Con A. The results obtained from divalent ligand **2** suggest that select low molecular weight ligands may serve as useful leads for the discovery of potent inhibitors or effectors.<sup>11,89,90</sup> Synthetic methods that accelerate the syntheses of multivalent low molecular weight compounds may facilitate the discovery of inhibitors and effectors of this class.

Synthetic multivalent ligands that cluster receptors may serve as potent effectors of biological function.<sup>1,12</sup> Additionally, a specific receptor type can be sensitive to different aspects of clustering, such as the number of receptors in a cluster, the rate at which the receptors are clustered, or the proximity between clustered receptors. To investigate relevant aspects of receptor clustering, we utilized three assays to examine Con A–multivalent ligand interactions. The resulting data suggest that different aspects of clustering can be independently influenced by multivalent ligand architecture. For example, dendrimeric

ligands rapidly induced Con A clustering, but the orientation of the receptor–ligand complexes did not allow for fluorescence quenching. This lack of quenching presumably results from unfavorable distances and orientations between receptors in the complexes that do not favor energy transfer, suggesting that dendrimeric scaffolds might not result in potent biological effectors. It is interesting to note that the protein conjugates used here were also not especially effective in clustering the target receptor. This result may be relevant as protein–antigen conjugates are used to raise immune responses, and their ability to promote B cell receptor clustering is likely an important determinant of their ability to elicit effective immune responses.

Specific applications of multivalent ligands may demand that the resulting receptor clusters have specific structural features. For example, searches for novel vaccine scaffolds may focus on materials that favor clustering large numbers of immune receptors.<sup>15</sup> Likewise, therapeutic strategies directed against bacterial toxins may benefit from multivalent ligands with an optimal potential for inhibiting protein binding.<sup>16,17,91,92</sup> These distinctions, however, are not always clear-cut. For example, ligands that cluster bacterial toxins may act at substoichiometric levels and, therefore, more effectively promote their clearance.<sup>51</sup> Our results suggest that control over the binding mechanism may be achieved by using specific multivalent ligand architectures.

The generality of the differences in ligand activities observed here is not known. Some attributes of the scaffolds described here that allow them to function as inhibitors or effectors are likely to be specific to the protein studied (Con A). Still, the polymers generated by ROMP, which are predicted to function as effectors from the assays used here, promote biological responses in a number of systems.<sup>1,19,21,98</sup> Further mechanistic investigations of receptor–multivalent ligand activity are needed to determine how the scaffold influences multivalent ligand-binding modes in different systems.

## Conclusions

Little is known about the relationships between multivalent ligand architecture and the mechanism(s) by which a given ligand engages receptors. Previous investigations addressing this question have focused on generating analogues within a single structural ligand class.<sup>87–90,93</sup> Although these approaches can yield materials with favorable activities, ligands with optimal activities for a variety of applications are unlikely to be identified from one structural class. We envisioned that ligands with diverse architectures would be required to identify access to these binding modes. Here, we dissect the activities of architecturally diverse multivalent ligands in four assays that explore individual aspects of receptor–ligand interactions.

- (87) Lynn, D. M.; Anderson, D. G.; Putnam, D.; Langer, R. *J. Am. Chem. Soc.* **2001**, *123*, 8155–8156.  
(88) Bosman, A. W.; Heumann, A.; Klaerner, G.; Benoit, D.; Fréchet, J. M. J.; Hawker, C. J. *J. Am. Chem. Soc.* **2001**, *123*, 6461–6462.  
(89) Goldberg, J.; Jin, Q.; Satoh, S.; Desharnais, J.; Capps, K.; Boger, D. L. *J. Am. Chem. Soc.* **2002**, *124*, 544–555.  
(90) Blackwell, H. E.; Clemons, P. A.; Schreiber, S. L. *Org. Lett.* **2001**, *3*, 1185–1188.

- (91) Mourez, M.; Kane, R. S.; Mogridge, J.; Metallo, S.; Deschatelets, P.; Sellman, B. R.; Whitesides, G. M.; Collier, R. J. *Nat. Biotechnol.* **2001**, *19*, 958–961.  
(92) Merritt, E. A.; Zhang, Z.; Pickens, J. C.; Ahn, M.; Hol, W. G. J.; Fan, E. *J. Am. Chem. Soc.* **2002**, *124*, 8818–8824.  
(93) Briehn, C. A.; Schiedel, M.-S.; Bonsen, E. M.; Schuhmann, W.; Bäuerle, P. *Angew. Chem., Int. Ed.* **2001**, *40*, 4680–4683.  
(94) Chernyak, A. Y.; Sharma, G. V. M.; Kononov, L. O.; Krishna, P. R.; Levinsky, A. B.; Kochetkov, N. K.; Rao, A. V. R. *Carbohydr. Res.* **1992**, *223*, 303–309.  
(95) Lindhorst, T. K.; Kieburg, C. *Angew. Chem., Int. Ed. Engl.* **1996**, *35*, 1953–1956.  
(96) Page, D.; Roy, R. *Bioconjugate Chem.* **1997**, *8*, 714–723.  
(97) Wu, P.; Brand, L. *Anal. Biochem.* **1994**, *218*, 1–13.  
(98) Gordon, E. J.; Sanders, W. J.; Kiessling, L. L. *Nature* **1998**, *392*, 30–31.

Individual assays provide information on only a limited number of binding modes. Because multivalent ligands can potentially access multiple binding modes, a single assay used in isolation is insufficient for understanding the mechanisms underlying multivalent ligand–receptor interactions. Here, we used four assays that report on various aspects of inhibitor and effector function. Moreover, the assays we employed are amenable to high-throughput, they involve minimal liquid-handling steps and small volumes. We anticipate that the identification of multivalent ligands with specific binding modes will benefit from the rapid analysis of candidates in multiple assays.

Our results suggest that the design of multivalent ligands for biological applications can benefit from combinatorial chemistry and diversity-oriented syntheses.<sup>11,89,90</sup> By varying ligand architecture, we were able to identify the mechanism of action preferred by a multivalent ligand. Our survey of 28 ligands from 5 different structural classes identified compounds that preferentially engage in selected binding modes. These results indicate that the study of the influence of ligand architecture on binding mechanisms will benefit from the investigation of a broad scope of structural combinations.

## Experimental Materials and Methods

**Ligand Synthesis.** Precursors to ligands **1–10** and **26–28** were obtained from commercial sources, as indicated. Mannose residues were appended to these scaffolds using the reagents 2-aminoethyl  $\beta$ -D-mannopyranoside, [*p*-isothiocyanato]-phenyl  $\alpha$ -D-mannopyranoside, or [2-isothiocyanato]-ethyl  $\alpha$ -D-mannopyranoside. These were generated from mannose using known procedures.<sup>94–96</sup> The concentrations of all ligands were calculated by hexose determination, as described,<sup>77</sup> using mannose as a standard. The concentrations of **7** and **26** could not be calculated in this fashion, as these ligands did not bear saccharide modifications. The concentration of these control compounds was determined by gravimetric or spectrophotometric analysis, and the concentrations employed corresponded to the maximum functionalized scaffold concentrations used (e.g., the concentration of **7** employed was the same as the concentration of **8**).

**1. Low Molecular Weight Compounds (1–4). A. Compound 1.** 2,2'-(Ethyleneoxy)bis(ethylamine) (3.2  $\mu$ L, 0.022 mmol, 1 equiv, Pierce, Inc., Rockford, IL) was reacted with [2-isothiocyanato]-ethyl  $\alpha$ -D-mannopyranoside (17.6 mg, 0.066 mmol, 2.5 equiv) in water. The product was dialyzed (100 molecular weight cutoff (mwco), 24 h, 4  $\times$  250 mL), and compound **1** was isolated as a solid (14.6 mg) in 98% yield. The product was purified by column chromatography using a 5:4:1 CH<sub>2</sub>Cl<sub>2</sub>/MeOH/H<sub>2</sub>O solvent system. <sup>1</sup>H NMR (300 MHz, 80% DMSO-*d*<sub>6</sub>, 20% D<sub>2</sub>O)  $\delta$  4.6 (s, 2H), 3.6–3.3 (m, 30 H), 1.2 (t, 4H). MALDI-TOF *m/z*: 701.4 [M<sup>+</sup>Na<sup>+</sup>] (M<sup>+</sup>Na<sup>+</sup> calcd 701).

**B. Compound 2.** 2,2'-(Ethyleneoxy)bis(ethylamine) (2.5  $\mu$ L, 0.0168 mmol, 1 equiv, Pierce, Inc., Rockford, IL) was treated with [*p*-isothiocyanato]-phenyl  $\alpha$ -D-mannopyranoside (12.3 mg, 0.042 mmol, 2.5 equiv) and triethylamine (7 mL, 0.0506 mmol, 3 equiv) in a methanol/water mixture (1:1 200  $\mu$ L total volume). The product was dialyzed (100 mwco, 24 h, 4  $\times$  250 mL), and compound **2** was isolated (4.7 mg) in 36% yield. <sup>1</sup>H NMR (300 MHz, 80% DMSO-*d*<sub>6</sub>, 20% D<sub>2</sub>O)  $\delta$  6.9 (s, 8H), 5.4 (d, 2H), 4.0 (m, 2H), 3.8 (dd, 2H), 3.6–3.4 (m, 20H). MALDI-TOF *m/z*: 797.3 [M<sup>+</sup>Na<sup>+</sup>] (M<sup>+</sup>Na<sup>+</sup> calcd 797).

**C. Compound 3.** Bis(sulfosuccinimidyl)suberate (5 mg, 0.00874 mmol, 1 equiv, Pierce, Inc., Rockford, IL) was treated with 2-aminoethyl  $\beta$ -D-mannopyranoside (7.79 mg, 0.0349 mmol, 4 equiv) in 200  $\mu$ L dimethyl sulfoxide (DMSO). The reaction was allowed to proceed for 3 h at 22 °C. Water was added to allow dialysis (500 mwco, 24 h, 2  $\times$  1000 mL). The resulting solution was lyophilized to afford compound **3** as a solid (4.2 mg) in 83% yield. <sup>1</sup>H NMR (300 MHz,

80% DMSO-*d*<sub>6</sub>, 20% D<sub>2</sub>O)  $\delta$  4.7 (s, 2H), 3.8–3.2 (m, 20H), 2.0 (m, 4H), 1.4 (m, 4H), 1.2 (s, 4H). MALDI-TOF *m/z*: 607.3 [M<sup>+</sup>Na<sup>+</sup>] (M<sup>+</sup>Na<sup>+</sup> calcd 605).

**D. Compound 4.** Tris(2-aminoethyl)amine (2.4  $\mu$ L, 0.0159 mmol, 1 equiv, Pierce, Inc., Rockford, IL) was reacted with [2-isothiocyanato]-ethyl  $\alpha$ -D-mannopyranoside (19 mg, 0.0717 mmol, 4.5 equiv) in water. The product was dialyzed (100 mwco, 24 h, 4  $\times$  250 mL), and compound **4** was purified by column chromatography using a 5:4:1 CH<sub>2</sub>Cl<sub>2</sub>/MeOH/H<sub>2</sub>O solvent system. Compound **4** was obtained as a solid (7.5 mg) in 50% yield. <sup>1</sup>H NMR (300 MHz, 80% DMSO-*d*<sub>6</sub>, 20% D<sub>2</sub>O)  $\delta$  4.6 (s, 2H), 3.6–3.4 (m, 18H), 3.3 (m, 18H), 2.6 (m, 12H). MALDI-TOF *m/z*: 964.4 [M<sup>+</sup>Na<sup>+</sup>] (M<sup>+</sup>Na<sup>+</sup> calcd 964).

**2. Dendrimers (5–6).** Starburst PAMAM dendrimers were obtained from Aldrich as 20 wt % solutions in methanol. Dendrimers **5** and **6** were prepared as described by Woller and Cloninger.<sup>24</sup> Compound **5**: <sup>1</sup>H NMR (300 MHz, 80% DMSO-*d*<sub>6</sub>, 20% D<sub>2</sub>O)  $\delta$  4.3 (s, 4H), 3.8–3.1 (m, 56H), 2.7 (m, 8H), 2.5 (s, 4H), 2.3 (m, 8H). MALDI-TOF *m/z*: 1577.7 [M<sup>+</sup>] (calcd 1577). Compound **6**: <sup>1</sup>H NMR (300 MHz, 80% DMSO-*d*<sub>6</sub>, 20% D<sub>2</sub>O)  $\delta$  4.6 (s, 8H), 3.8–3.2 (m, 48H), 3.1 (m, 48H), 2.7–2.5 (m, 36H), 2.4–2.0 (m, 48H). MALDI-TOF *m/z*: 3312.8 [M<sup>+</sup>] (M<sup>+</sup> calcd 3552–242 = 3310, one unreacted site).

**3. Globular Protein Conjugates (7–10).** A thiol was appended to 2-aminoethyl  $\beta$ -D-mannopyranoside (3 mg/mL in DMSO) by reaction with the *N*-hydroxysuccinimidyl ester of *S*-acetylthioacetic acid (SATA, 2 equiv, Pierce, Inc., Rockford, IL). The reaction was conducted for 2 h at 22 °C. Remaining SATA was removed by scavenger resin (100-fold molar excess of amines). After the removal of the resin, the thioester was treated with 0.5 M hydroxylamine (100  $\mu$ L, 10 mM phosphate buffer, 25 mM EDTA, pH 7.2, 15 min) to reveal the thiol group. The thiol-containing mannose derivative was added to 10 mg/mL IMJECT BSA (maleimide-activated bovine serum albumin, Pierce, Inc., Rockford, IL) in phosphate buffered saline (PBS) at pH 7.1. IMJECT BSA contains approximately 20 maleimides per BSA, according to manufacturer specifications. Mannosylation reactions were performed for 2 h at 22 °C on a rotary shaker. Cysteine (100  $\mu$ L, 30  $\mu$ M) was added to quench the unreacted maleimides. Shaking was continued for 1 h at 22 °C. The resulting solution was dialyzed (7000 mwco, 2  $\times$  1000 mL) overnight against 10 mM HBS (10 mM HEPES, 150 mM NaCl, pH 7.5). Compounds **8–10** were isolated. Control compound **7** was not treated with 2-aminoethyl  $\beta$ -D-mannopyranoside but, otherwise, received identical treatment.

**4. Linear Defined Polymers (11–25).** The syntheses and characterization of **11–25** are reported elsewhere.<sup>22,29</sup> Polymer length (*n*) was estimated by integration of <sup>1</sup>H NMR peaks.

**5. Polydisperse Polymers (26–28).** 2-Aminoethyl  $\beta$ -D-mannopyranoside (4.42 mg, 0.5 equiv, 0.1 mg/mL) and polyethylene maleic-anhydride (PEMA) polymers (10 mg, 35 mg/mL, Polysciences Inc., Warrington, PA) were dissolved in DMSO. The PEMA was considered to be an average molecular weight of 100 000 (according to manufacturer specifications), which constitutes an average of 400 maleic anhydride and 400 ethylene units per polymer chain. The conjugation reaction was agitated for 3 h at 22 °C on a rotary shaker. The remaining maleic anhydride groups were quenched with the addition of 100  $\mu$ L of distilled water, and the product was treated with a 2-fold molar excess of trimethylsilyldiazomethane to methylate any carboxylic acid groups. Solutions were brought to <25% DMSO by the addition of distilled water, dialyzed overnight (7000 mwco, 2  $\times$  1000 mL), and compound **28** was isolated. Similar conditions were used to generate compound **27**. Control polymer **26** was generated by the addition of ethanolamine in place of the mannose-derivative.

**Solid-Phase Binding Assay.** Microtiter well plates activated with maleic anhydride (Reacti-bind polystyrene 96-well plates, Pierce, Inc.) were derivatized with mannose by the addition of a solution of 2-aminoethyl  $\beta$ -D-mannopyranoside (50  $\mu$ L, 1 mg/mL) in HBS. Plates were incubated for 60 min at 22 °C. Wells were washed twice with phosphate-buffered saline containing 0.1% Tween-20 and 1 mM CaCl<sub>2</sub>

(PBST-Ca<sup>2+</sup>). Solutions of 50  $\mu\text{g}/\text{mL}$  fluoresceinated Con A (Vector Laboratories, Burlingame, CA) and mannose-bearing ligands **1–28** in PBST-Ca<sup>2+</sup> were incubated in the wells for 30 min at 22 °C. Wells were washed twice with PBST-Ca<sup>2+</sup> and once with HBS. Remaining fluoresceinated Con A was detached for analysis by the addition of 100  $\mu\text{L}$  of 100 mM methyl  $\alpha$ -D-mannopyranoside. After a 15 min incubation, these solutions were transferred to cluster plates (Costar black with clear bottom cluster plate, Corning Inc., Corning NY) suitable for fluorescence analysis. Fluorescein emission intensity was determined on a BioLumin plate reader using 5-nm slit widths, a PMT voltage of 850 V, an excitation wavelength of 480 nm, and an emission wavelength of 520 nm.

**Quantitative Precipitation.** Quantitative precipitation experiments were carried out and interpreted as described previously.<sup>49,51</sup> All ligands were diluted in distilled water. Trace amounts of DMSO had a negligible effect on the results of this assay.

**Turbidity Assay.** This assay was performed as described previously.<sup>29,31</sup> Briefly, Con A was diluted to 5  $\mu\text{M}$  Con A tetramers in HBS, and the ligand of interest was added to a final concentration of 50  $\mu\text{M}$ . The solution was mixed vigorously for 5 s using a micropipet and then placed in the spectrometer. Absorbance data was recorded at 420 nm for 10 min at 1 Hz.

**Fluorescence Quenching Assay.** The fluorescence quenching experiments were performed with some minor modifications to the procedure described previously.<sup>50,51</sup> The modifications were made to allow a more rapid analysis of samples in 96-well plates. Con A derivatives labeled with donor and acceptor fluorophores (4  $\mu\text{g}/\text{mL}$  of fluoresceinated and rhodamine-labeled Con A, Vector Laboratories,

Burlingame, CA) and ligand were added to the wells of black cluster plates in a final volume of 100  $\mu\text{L}$ . The buffer was calcium-enriched HBS (HBS + 1 mM CaCl<sub>2</sub>). Solutions were mixed by gentle tapping and then incubated at 22 °C for 30 min in the dark. Fluorescein emission was measured on a BioLumin plate reader using 5-nm slit widths, a PMT voltage of 850 V, an excitation wavelength of 485 nm, and an emission wavelength of 520 nm. Ligands had negligible fluorescence at 520 nm (data not shown). Half-maximal fluorescence values were determined by fitting data to nonlinear curves.<sup>97</sup>

**Acknowledgment.** We acknowledge Prof. P. Friesen (UW-Madison) for the generous access to equipment. Synthetic intermediates were supplied by Dr. M. Kanai, Dr. M. C. Schuster, and R. M. Owen. This research was supported in part by the NIH (GM 49975) and by the Keck Foundation (center for Chemical Genomics). J.E.G. thanks the NIH-sponsored Biotechnology Training Program for a predoctoral fellowship (GM 08349). L.E.S. was supported by an NIH predoctoral fellowship (GM 18750). K.A.O. was supported by a Trewartha Honors Undergraduate Fellowship from UW-Madison.

**Supporting Information Available:** NMR data for multivalent ligands and raw and processed data for solid-phase binding assay, turbidity assay, quantitative precipitation assay, and fluorescence quenching assay. This material is available free of charge via the Internet at <http://pubs.acs.org>.

JA027184X